Journal of Alloys and Compounds 504S (2010) S56–S59

Contents lists available at ScienceDirect

Journal of Alloys and Compounds

journal homepage: www.elsevier.com/locate/jallcom

Multi-scale modeling of shear banding in iron-based metallic glasses

G.P. Zheng*, Y. Shen

Department of Mechanical Engineering, The Hong Kong Polytechnic University, Hung Hom, Kowloon, Hong Kong

ARTICLE INFO

Article history:
Received 2 July 2009
Received in revised form
22 December 2009
Accepted 25 February 2010
Available online 10 March 2010

Keywords:
Metallic glasses
Atomic scale structure
Computer simulations

ABSTRACT

Multi-scale modeling approaches are developed to investigate the deformation mechanisms in iron-based metallic glasses. The shear band formation and crack propagation in the iron-based metallic glasses are investigated using a phase-field phenomenological model. The parameters which are necessary to the formulism of mesoscopic phase-field modeling, e.g., the surface energy, activation energy and elastic constants related to the formation of free-volume defects, are obtained by *ab initio* molecular dynamics simulations on an amorphous $Fe_{80}Si_{10}B_{10}$ model system. The important features of shear banding such as shear band width and crack propagation velocity obtained from the multi-scale modeling are consistent with those of experiments. These results demonstrate that the mechanical behaviors of bulk metallic glasses can be understood by the multi-scale modeling developed in this study.

1. Introduction

Although iron-based metallic glasses have been invented for more than 30 years [1], there are increasing interests in the iron-based bulk metallic glasses (BMGs) with typical sizes larger than several millimeters [2]. The iron-based BMGs are superior to their BMG counterparts because theoretically they would possess larger strength and because their main content iron is relatively cheap. However they are very brittle [2] since the deformation of these glassy alloys is localized in nature. For structural applications, iron-based BMGs with excellent combination of mechanical properties have to be developed based on the description, characterization and prediction of their deformation behaviors. But up to date our understanding of the deformation mechanisms of these glassy alloys is very limited and incomplete [3].

One of the major obstacles that prevent us from comprehensive understanding of the deformation mechanism of glassy alloys is their atomistic deformation defects [4]. Unlike crystalline iron alloys, iron-based BMGs do not have dislocation defects during the deformation process and the deformation is executed by the activation or creation of free-volume defects [5] within a region with sizes smaller than 1 nm, which is described as shear transformation zone (STZ) [6]. The shear banding is a result of the formation or coalescences of STZs depending on the local stress states, temperature, and other structural entities such as voids and chemical heterogeneities.

Despite encouraging progresses in the characterization of STZ, successful applications of the free-volume activation theory in the description and modeling of various shear banding phenomena observed in experiments are still very limit. In this study, we develop multi-scale approaches to model shear band initialization and propagation based on the quantitative descriptions of energetics and kinetics of free-volume defects, using Fe–Si–B metallic glass ribbon as an example. In the atomic scale, the surface energy, activation energy and elastic constants related to the formation of free-volume defects are obtained by *ab initio* molecular dynamics (AIMD) simulations. These physical quantities are then used to construct the energy landscape of a metallic glass consisting of free-volume defects. Finally the shear banding in the deformed glassy alloy is investigated by solving the kinetic governing equations or phase-field equations of the system in the mesoscopic scale. The shear banding behaviors in the atomic length scale and in mesoscopic length scale are thus successfully bridged.

2. AIMD simulation on deformation behaviors of Fe–Si–B metallic glasses

Simulation of $Fe_{80}Si_{10}B_{10}$ metallic glass is performed using the first-principles simulation code VASP [7]. Generalized gradient approximation for the exchange-correlation energy and the spin-polarized projector augmented-wave method is implemented. Kohn-Sham single electron wave functions are expanded by plane waves with well-converged cut-off energy of 400 eV. The supercell contains 200 atoms and the period boundary conditions (PBC) are used for all calculations. The Brillouin zone sampling consists of the Γ point only. The metallic glass is prepared by quenching the melt

* Corresponding author.
E-mail address: mmzheng@polyu.edu.hk (G.P. Zheng).

0925-8388/$ – see front matter © 2010 Elsevier B.V. All rights reserved.
doi:10.1016/j.jallcom.2010.02.165

Table 1
Comparison of density ρ_0, shear modulus μ, bulk modulus B, Poisson's ratio ν and magnetic moment per iron atom m between Fe–Si–B model system and experiments [7,8].

	ρ_0 (kg/m^3)	μ (GPa)	B (GPa)	ν	m (μ_B)
AIMD simulation	7.383	60.1	161.4	0.33	2.05
Experiments	7.392	58.2	162.7	0.34	2.04

to room temperature. The starting configuration of the Fe–Si–B system for AIMD simulation is generated by classical MD simulation of Fe–Si–B using hard sphere potentials. The system is first melted at $T = 1500$ K for 5 ps and is then quenched to $T = 650$ K with a cooling rate of 2×10^{14} K/s. The system with a density of 7.02 kg/m^3 is maintained as undercooled liquid for 1.5 ps, following by the quenching to $T = 300$ K with a quenching rate of 4×10^{14} K/s. All the MD simulations are performed in the canonical (NVT) ensemble and Nose thermostat is used for temperature control. A stable glassy $Fe_{80}Si_{10}B_{10}$ system is finally obtained by the relaxations of atomic coordinates and supercell volume using the conjugate gradient algorithm at $T = 0$ K. The tolerances of 1.0 meV for maximal change in total energy and 10 MPa for maximal change in stress components are used to determine a stable glassy system, where all the deformations are performed.

Some physical properties of the glassy $Fe_{80}Si_{10}B_{10}$ are listed in Table 1. The shear modulus is calculated by rigid shear of the system and the bulk modulus is calculated from the pressure–volume relation. There are all in good agreement with experimental results [8,9]. We also calculate the pair distribution function of the system and it is consistent with experiments. In addition, the cluster environment of atoms evaluated by Voronoi polyhedron analysis shows that there are no signatures of bcc or fcc crystalline structures in the system. All these results suggest that the model system is in fully amorphous state.

Tensile deformation and shear deformation in the glassy alloy are performed, which simulate mode-I and mode-II fracture processes, respectively. The schematics are illustrated in the insets of Fig. 1 and the fracture (YZ) plane is represented by the green solid line. In the tensile deformation, glassy alloys at both sides of the fracture plane are separated by a distance Δx and atoms are not allowed to relax. In the shear deformation, a relative displacement Δy between glassy alloys at both sides of the fracture plane is imposed along the fracture plane. In this case, the y- and z-coordinates of each atom are fixed in each ionic step of AIMD and the atoms are relaxed only along the direction (x-) perpendicular to the fracture plane. Fig. 1(a) and (b) shows the total free energy of the systems under tension and shear deformations, respectively.

From Fig. 1(a) we can determine the surface energy of glassy alloy to be $\gamma_s = 1.6$ J/m^2 which equals to the energy necessary to create two fracture surfaces (with an area $A = 1.07$ nm^2) of the left and the right parts of the glassy system. In Fig. 1(a) we notice that the stress along the tensile direction shows a maximum before fracture occurs, which indicates the activation of STZ. Based on the free-volume model, we can define the surface energy of free-volume defect to be $\gamma_f = 0.51$ J/m^2.

Because of PBC, the shear deformation will not result in fracture surfaces. This feature allows us to estimate the activation energy of free-volume defects. In Fig. 1(b) we can find that within a shearing distance of 0.204 nm the energy change of the system does not excess 0.01 eV. A sharp energy barrier of $\Delta U = 5.4$ eV has to be overcome if the glassy alloy would be further deformed. The existence of a large energy barrier demonstrates that the STZ-induced heterogeneous deformation is the deformation mechanism of metallic glass at low temperature, which is first proposed by Argon [5]. Hence $\Delta U = 5.4$ eV is a fair estimate of the activation energy of free-volume defect.

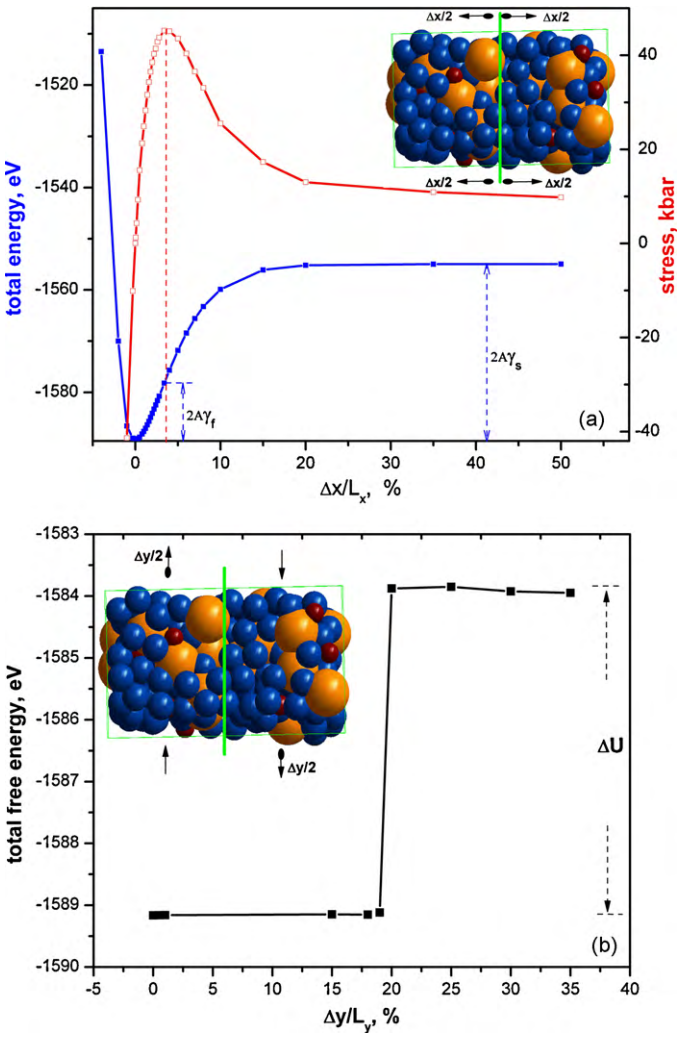

Fig. 1. (a) Free energy and stress of the model Fe–Si–B glassy alloy under tensile deformation. The inset is the schematic. The solid green line denotes the fracture plane. Alloys at both sides of the plane are separated along the x-direction, and $L_x = 2.036$ nm. (b) Free energy of glassy alloy under shear deformation. Alloys at both sides of the plane are sheared along the y-direction. $L_y = 1.34$ nm. (For interpretation of the references to color in this figure legend, the reader is referred to the web version of the article.)

3. Continuum modeling of shear banding by phase-field phenomenological model

The physical quantities obtained by AIMD simulation of deformed metallic glass enable us to construct the energy landscape of a metallic glass consisting of free-volume defects. The model is based on the definition of coarse-grained phase field for free-volume distribution [10]. The free-volume density is defined as $\rho(\vec{r}) = (v_i - v_0)/(v_m - v_0)$, where v_m is the maximum dilated volume when complete decohesion occurs at position $\boldsymbol{r}$, v_i is the atomic volume defined as the volume of the so-called Voronoi polyhedron of the ith atom, v_0 is the atomic volume in the undeformed ideal random close packing state. The free-energy functional of the metallic glass is written as [11]

$$F = \int \left\{ f(\rho, \varepsilon_{ij}) + \frac{\rho_0}{2}[\dot{\vec{u}}]^2 + \frac{\kappa}{2}|\vec{\nabla}\rho|^2 \right\} dV, \tag{1}$$

where

$$f(\rho, \varepsilon_{ij}) = e[\varepsilon_{ij}] + \frac{a_0}{2}\rho^2 + \frac{b_0}{3}\rho^3 + \frac{c_0}{4}\rho^4 + \left(\frac{a_1}{2}\rho^2 + \frac{b_1}{3}\rho^3\right)(e[\varepsilon_{ij}] - e_0), \tag{2}$$

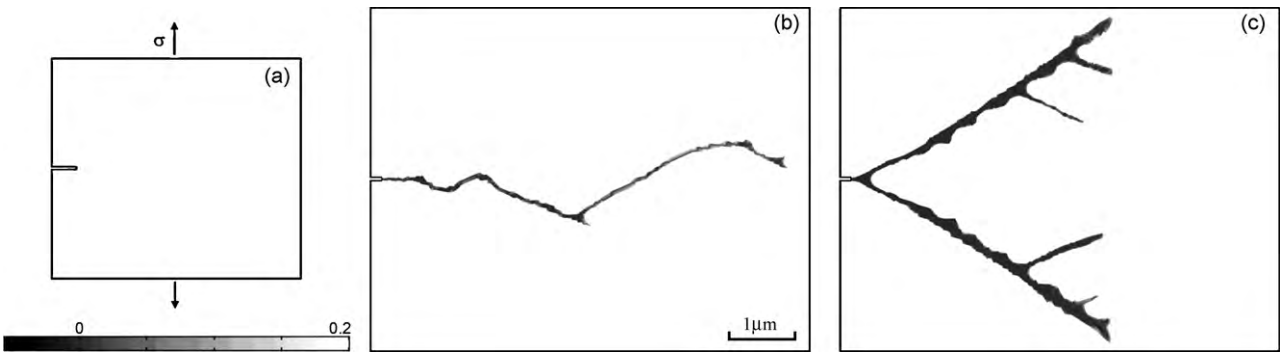

Fig. 2. (a) Phase-field model for amorphous Fe–Si–B metallic ribbon. A uniaxial tensile stress is applied along the *y*-direction. (b and c) Shear bands under stress intensity factors $K = 44.1$ and $117.6\ \mathrm{MPa(m)}^{1/2}$, respectively. Only a strip of the ribbon is shown. The gray scales correspond to the free-volume density values of $1-\rho$.

$$e[\varepsilon_{ij}] = \frac{1}{2}C_{ijkl}\varepsilon_{kl}\varepsilon_{ij}$$
$$C_{ijkl} = \mu(\delta_{ik}\delta_{jl}+\delta_{il}\delta_{jk})+\lambda\delta_{ik}\delta_{jl} \quad (3)$$

and ε_{ij} is the strain tensor defined by the displacement field **u** through the relation $\varepsilon_{ij} = (\partial u_j/\partial x_i + \partial u_i/\partial x_j)/2$; λ is Lamé coefficient related to the bulk modulus B by $B = \lambda + 2\mu/3$. e_0 is the strain energy at the elastic limit. The gradient term of free-volume density in Eq. (1) measures the "interfacial" energy between the deformed and undeformed regions and is defined as $\kappa = \gamma_f R$ where R is a macroscopic length scale for shear band and could be measured from experiments.

The $Fe_{80}Si_{10}B_{10}$ under a mode-I cracking at $T = 300$ K is simulated by solving the equations for ρ and **u** written as follows:

$$\tau_\rho \frac{\partial \rho}{\partial t} = -\frac{\delta F}{\delta \rho} = \kappa\nabla^2\rho - (a_0\rho + b_0\rho^2 + c_0\rho^3) - \rho(a_1 + b_1\rho)(e[\varepsilon_{ij}] - e_0), \quad (4)$$

$$\rho_0 \frac{\partial^2 \vec{u}}{\partial t^2} = -\nabla\cdot\left[\frac{\delta F}{\delta \varepsilon_{ij}}\right] = \mu\nabla\cdot\left\{\left[1+\rho^2\left(\frac{a_1}{2}+\frac{b_1}{3}\rho\right)\right]\nabla\vec{u}\right\}, \quad (5)$$

where $\tau_\rho = 0.2$ ns is the characteristic time for free-volume activation. We use experiment data $T_g = 620$ K, $R = 0.5\ \mu$m and fracture strain $\varepsilon_f \sim 1.8\%$. The coefficients are given by $a_0 = 4(2 - T/T_g)\Delta U$, $b_0 = -32\Delta U$, $c_0 = 16\Delta U$ and we choose $a_1 = 4$ and $b_1 = -9$. We define that a shear band forms in a region where $\rho > \rho_c = 0.8$.

The dimensions of a $Fe_{80}Si_{10}B_{10}$ ribbon are $20\ \mu\mathrm{m} \times 20\ \mu\mathrm{m} \times 5\ \mu\mathrm{m}$. As shown in Fig. 2(a), there is an initial rectangular crack with a length $l = 0.4\ \mu$m and a width of $0.04\ \mu$m. The shear banding is successfully captured by the phase-field model, and we find that the shear band can be initiated from the initial crack when the stress intensity factor reaches $K = \sigma\sqrt{l\pi} = 40.3\ \mathrm{MPa(m)}^{1/2}$. When $K > K_{IC} = 44.1\ \mathrm{MPa(m)}^{1/2}$ the crack starts to propagate, resulting in either wavy cracks (Fig. 2b) or highly bifurcated cracks (Fig. 2c). These results are consistent with the experimental observation of the mode-I cracking of glassy Fe–Si–B ribbon [3]. The fracture toughness K_{IC} estimated from the modeling is also comparable with that measured in $Fe_{80}Si_{10}B_{10}$ metallic glass [3].

Combined with the first-principles calculation of the parameters necessary to construct the free-energy functional (Eq. (1)), the phase-field continuum modeling thus provides us a useful tool to investigate the shear banding in the metallic glass under plastic deformation. One of the important immediate applications is to characterize the shear band thickness and the stress state near the shear band. It is general believed that shear bands are the only region of metallic glass to suspend the plastic deformation. Characterization of the micromechanics of shear band would allow us to quantitatively relate the microscopic shear banding to the macroscopic mechanical behaviors of materials.

As shown in Fig. 3(a), we measure the relative shear band thickness $\Delta w/w$ and the shear stress τ near the shear band, where Δw is defined as the change of shear band thickness during the advance

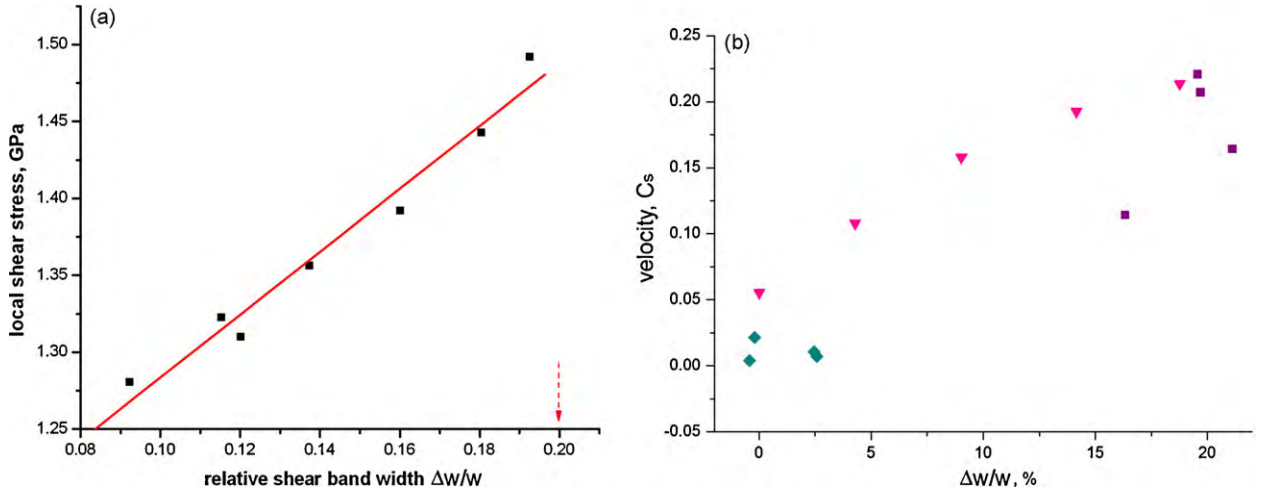

Fig. 3. (a) Shear stresses around the shear bands at various relative shear band thicknesses $\Delta w/w$. The solid line is the fit of Eq. (6). (b) Relationship between shear band velocity and relative shear band thickness $\Delta w/w$. C_s is the shear wave speed. The diamond, triangle and square symbols represent shear band initialization, propagation and bifurcation, respectively.

of shear band along its propagation direction with a distance w. The relation between τ and $\Delta w/w$ is linear and is expressed as

$$\tau = 2.04 + 1.08\frac{\Delta w}{w} \ (\text{GPa}) \quad (6)$$

The arrow in Fig. 3(a) indicates the upper limit of $\Delta w/w$ in Eq. (6). Shear band bifurcation occurs when $\Delta w/w > 0.2$. It can be found in Eq. (6) that the critical shear stress to initial a shear band is 2.04 GPa corresponding to $\Delta w/w = 0$, which is comparable with the flow strength (3.8 GPa) from experimental measurement [8].

Another important application of the multi-scale modeling is to investigate the shear band kinetics. Fig. 3(b) shows the variation of shear band velocity with relative shear band thickness $\Delta w/w$. There are three stages of shear band movement as shown in Fig. 3(b), i.e., initiation and propagation, growth and bifurcation. It is shown in Fig. 3(b) that the shear band attains its maximum velocity when the bifurcation occurs. Because shear band branching or bifurcation is close related to macroscopically observed deformation behavior of serrated flow which is strain-rate dependent, it is suggested the shear band kinetics can be used to interpret such unique and important deformation characteristics in metallic glasses.

4. Concluding remarks

Multi-scale modeling methods are developed to investigate the shear banding in iron-based metallic glasses. We first calculate in atomic scale the physical quantities such as the surface energy, activation energy and elastic constants that are related to the formation of free-volume defects using density functional theory. The free-energy functional of a metallic glass consisting of free-volume defects is then constructed and the deformation behaviors of the metallic glass are modeled by the mesoscopic phase-field model. The mechanical properties such as fracture toughness and yield strength of Fe–Si–B glassy alloys obtained from the simulation are in good agreement with experiments. In particular, using these multi-scale approaches, shear banding phenomenon and kinetics are quantitatively characterized, which have not been comprehensively investigated by any other simulation methods up to date. Because the approaches developed in this study are general, they are not restricted to simulate iron-based metallic glass in atomistic and mesoscopic scales. Instead they can be used to investigate the deformation behaviors of other glassy alloy systems and glass alloys with larger sizes such as BMGs.

Acknowledgements

The work described in this paper was supported by a grant from the Research Grants Council of the Hong Kong Special Administrative Region, China (Project No. PolyU 7196/06E). The authors are grateful for the supports provided by the Research Funds of Hong Kong Polytechnic University (Project No. G-YH33).

References

[1] P. Duwez, in: H.-J. Guntherodt, H. Beck (Eds.), Glassy Metals I, Springer-Verlag, Berlin, 1981, p. 19.
[2] V. Ponnambalam, S.J. Poon, G.J. Shiflet, V.M. Keppens, R. Taylor, G. Petculescu, Appl. Phys. Lett. 83 (2003) 1131;
C. Changa, T. Kubota, A. Makino, A. Inoue, J. Alloys Compd. 473 (2009) 368.
[3] C.A. Pampillo, J. Mater. Sci. 10 (1975) 1194.
[4] F. Spaepen, Acta Metall. 25 (1977) 407.
[5] A.S. Argon, Acta Metall. 27 (1979) 47.
[6] M.L. Falk, J.S. Langer, Phys. Rev. E 57 (1998) 7192.
[7] G. Kresse, J. Furthmüller, Phys. Rev. B 54 (1996) 11169.
[8] A. Inoue, H.S. Chen, J.T. Krause, T. Masumoto, M. Hagiwara, Science Report of the Research Institute of Tohoku University, vol. 31A, 1983, p. 124.
[9] J. Durand, M. Yung, in: R.A. Levy, R. Hasegawa (Eds.), Amorphous Magnetism II, Plenum Press, New York, 1977, p. 275.
[10] G.P. Zheng, Ph.D. thesis, Johns Hopkins University, 2002.
[11] G.P. Zheng, M. Li, Phys. Rev. B 80 (2009) 104201.